

Hubble Space Telescope imaging survey of sub-mJy star-forming galaxies I: morphologies at $z \sim 0.2$

Stephen Serjeant¹, Bahram Mobasher^{1,2,3}, Carlotta Gruppioni^{1,4}, Seb Oliver^{1,5}

¹*Astrophysics Group, Blackett Laboratory, Imperial College, Prince Consort Road, London SW7 2BZ, UK*

²*Space Telescope Science Institute, 3700 San Martin Drive, Baltimore, MD 21218, USA*

³*Affiliated with the Astrophysics Division, European Space Agency*

⁴*Osservatorio Astronomico di Bologna, via Ranzani 1, 40127 Bologna, ITALY*

⁵*Astronomy Centre, CPES, University of Sussex, Falmer, Brighton BN1 9QJ*

Accepted; Received; in original form 1999 Jan 31

ABSTRACT

We present the first results of our HST WFPC2 F814W snapshot imaging survey, targeting virtually all sub-mJy decimetric radio-selected star-forming galaxies. The radio selection at ~ 1 GHz is free from extinction effects and the radio luminosities are largely unaffected by AGN contamination, making these galaxies ideal tracers of the cosmic star formation history. A sub-sample of 4 targets is presented here, selected at 1.4 GHz from the spectroscopically homogenous and complete samples of Benn et al. (1993) and Hopkins et al. (1999). The redshifts are confined to a narrow range around $z \sim 0.2$, to avoid differential evolution, with a radio luminosity close to L_* where the galaxies dominate the comoving volume-averaged star formation rate. We find clearly disturbed morphologies resembling those of ultraluminous infrared galaxies, indicating that galaxy interactions may be the dominant mechanism for triggering star formation at these epochs. The morphologies are also clearly different from coeval quasars and radiogalaxies, as found in star-forming galaxies selected at other wavelengths. This may prove challenging for models which propose direct causal links between AGN evolution and the cosmic star formation history at these epochs. The asymmetries are typically much larger than seen in the CFRS at similar redshifts, optical luminosities and $H\alpha$ -derived star formation rates, indicating the possible existence of an obscuration-related morphological bias in such samples.

Key words: cosmology: observations - galaxies: formation - infrared: galaxies - surveys - galaxies: evolution - galaxies: star-burst

1 INTRODUCTION

The study of the observational constraints on the cosmic star formation history is currently among the most active fields in observational cosmology. The most widely used tracer of the comoving volume-averaged star formation rate (SFR) is the UV luminosity density (e.g. Madau et al. 1996, Steidel et al. 1996, 1999), found to peak at $z \sim 1 - 2$. However, little is known about the history of star formation in the Universe beyond its global average (e.g. Abraham

et al. 1999). In this paper we present the first results from an on-going program with Hubble Space Telescope (HST) to study the morphology of starforming galaxies, using a sample of galaxies which dominate the comoving SFR and which were selected in a manner free from obscuration biases.

An important caveat to the SFR constraints is that the UV luminosity of star-forming galaxies is dominated by the lowest-extinction regions. This leads to extreme sensitivity to obscuration corrections

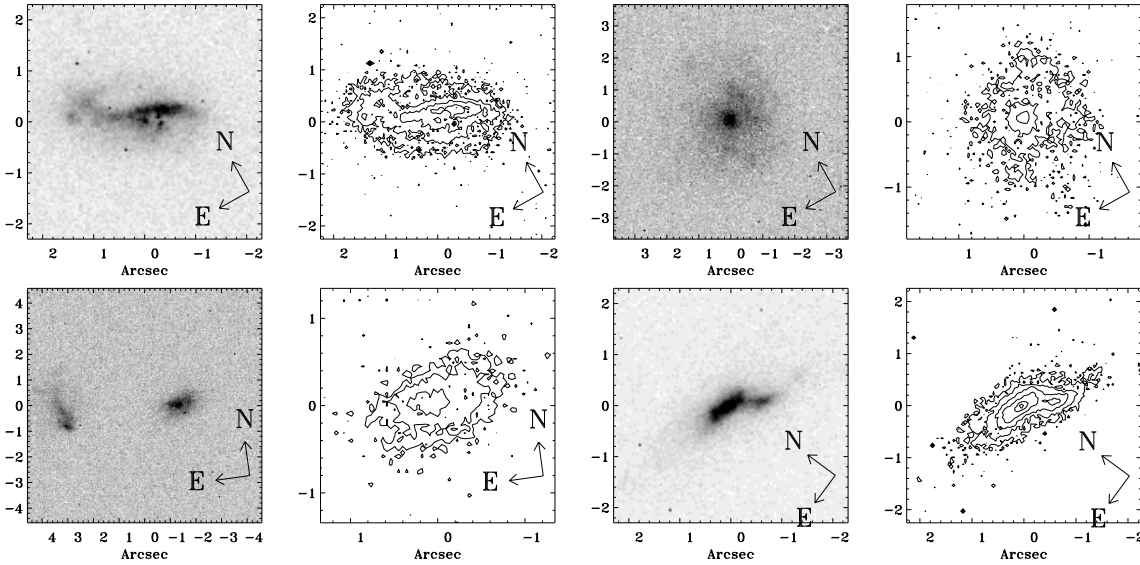


Figure 1. HST F814W snapshots of the galaxies [CM84]144 (top left), [CM84]074 (top right), Phoenix-Deep-29 (bottom left) and Phoenix-Deep-96 (bottom right). Greyscale is linear, and contours are spaced in factors of 2.

Name	RA (J2000)	Dec (J2000)	Mag	z	$S_{1.4}$ (mJy)	I_{814}	M_B (AB)	SFR (1.4)	SFR ($H\alpha$)	A
[CM84]144 ^{2,3,4}	08 55 47.60	+17 02 28.4	B = 18.7	0.2253	0.29	18.3	-21.2	116.3	12.9	0.47
[CM84]074 ^{2,3,4}	08 54 58.33	+17 03 46.9	B = 18.6	0.2279	0.29	18.7	-20.8	117.6	8.34	0.112
Phoenix-Deep-29 ^{1,5,6}	01 10 43.88	-45 51 22.7	R = 20.2	0.210	0.198	19.7	-19.6	52.5	1.1	0.185
Phoenix-Deep-96 ^{1,5,6}	01 12 25.21	-45 47 0.1	R = 18.4	0.236	0.225	18.3	-21.2	75.9	31.0	0.317

Table 2. HST $z \sim 0.2$ sub-mJy star-forming snapshot sample observed to date. All were observed for 2×400 seconds with the PC in filter F814W. References are (1) Georgakakis et al. 2000, (2) Condon & Mitchell 1984, (3) Rowan-Robinson et al. 1993, (4) Benn et al. 1993, (5) Hopkins et al. 1998, (6) Hopkins et al. 1999. Star formation rates (1.4 GHz and $H\alpha$) are in $M_\odot \text{ yr}^{-1}$, and A are the asymmetries. For comparison, the $z = 0.2$ ($z = 0.3$) radio L_* assuming $(1+z)^3$ luminosity evolution corresponds to $63.4 M_\odot \text{ yr}^{-1}$ ($80.6 M_\odot \text{ yr}^{-1}$). The Tresse & Maddox (1997) $H\alpha L_*$ at $z \sim 0.2$ corresponds to $22.4 M_\odot \text{ yr}^{-1}$.

Redshift	Evolution	L_* 1.4 GHz Flux
0.2	$(1+z)^3$	0.264 mJy
0.2	none	0.153 mJy
0.3	$(1+z)^3$	0.145 mJy
0.3	none	0.066 mJy

Table 1. Flux of the break in the 1.4 GHz luminosity function (L_*) under various luminosity evolution assumptions. Uses the luminosity function from Serjeant et al. 1998, with an $\Omega = 1$, $\Lambda = 0$ world model. Very similar results are derived from the Condon 1992 luminosity function. For a Hubble constant of $H_0 = 50 \text{ km s}^{-1} \text{ Mpc}^{-1}$ the characteristic luminosity lies at $\sim 2.8 \times 10^{22} \text{ W Hz}^{-1}$. The fluxes themselves are H_0 -independent.

(e.g. Pettini et al. 1998, Meurer et al. 1997), large enough to eliminate the evidence for a redshift cut-off in the SFR. Indeed, SCUBA observations of the Hubble Deep Field (HDF) (Hughes et al. 1998) detected 5 ultraluminous galaxies at $z > 2$ (the redshift constraints come mainly from the radio-FIR correlation

and not from the uncertain HDF IDs), which together implied an obscured star formation rate at least as large as the integrated de-reddened UV-derived rate. Moreover, the $H\alpha$ -derived star formation rate from the Canada-France Redshift Survey (CFRS, Tresse & Maddox 1997) was a factor $\sim \times 3$ larger than the UV estimate in the same sample, but comparable to those derived from the mid-IR for the CFRS (Flores et al. 1999) or the HDF (Rowan-Robinson et al. 1997).

However, a serious problem is that optical-UV light is strongly skewed to low extinction regions, while the reverse is true for mid and far-IR selected samples, leading to problematic obscuration-related effects in either case. An unbiased technique for selecting star-forming galaxies is to sample at decimetric radio wavelengths, where both obscured and unobscured star forming galaxies contribute (Condon 1992). Several groups (including ourselves) have begun to exploit this technique to trace the cosmic star formation history, and to study the obscuration effects in star forming galaxies (e.g. Cram et al. 1998,

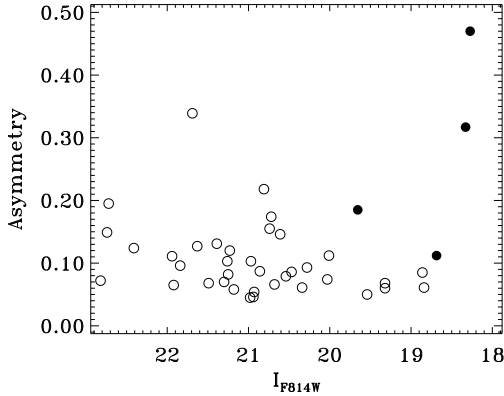


Figure 2. Asymmetry parameters for the radio-selected sub-mJy star-forming galaxies (filled symbols) compared to the CFRS/LDSS galaxies with $0.17 \leq z \leq 0.3$ (open symbols).

Serjeant et al. 1998, Oliver et al. 1998, Haarsma & Partridge 1998, Cram 1998, etc).

We have embarked on a programme to image almost all star-forming galaxies selected at decimetric radio wavelengths, using the WFPC2 in snapshot mode on the HST. In this paper we carry out a morphological study of a small subset of these galaxies at $z \sim 0.2$, from our first cycle 8 observations in this programme. (Although these are at low redshifts by many standards, they are *not* local, with the volume-averaged SFR being a factor of $\sim \times 2$ higher than in the local Universe for $(1+z)^3$ luminosity evolution models (Table 1).) The galaxies in this sample are selected so that they dominate the (radio-derived) star formation history of the Universe at this epoch, i.e. close to the L_* characteristic luminosity in the radio luminosity function.

The sample selection is discussed in Section 2, which also presents the HST observations and data reduction. These data are then analysed in Section 3, followed by a discussion of the results in Section 4.

2 SAMPLE SELECTION AND OBSERVATIONS

The following criteria are considered in selecting the sample for HST observations:

(i) The objects are sub-mJy radio sources, selected at 1.4 GHz (Benn et al (1993); Georgakakis et al (2000)). This avoids obscuration-related selection biases. Decimetric radio fluxes are much less affected by AGN contribution than shorter wavelength observations (compare e.g. the ongoing controversy over the AGN fraction in higher frequency sample with Hammer et al. (1995) finding $\sim 50\%$ AGN fraction at 5–8 GHz while Windhorst et al. (1995) find only $\sim 5\%$).

(ii) Spectroscopic data are used to select emission-line star-forming galaxies.

(iii) The galaxies must not lie close to bright stars to avoid HST roll angle constraints.

(iv) Galaxies selected to lie close to the 1.4GHz L_* , which dominate the volume averaged SFR (Table 1).

(v) Galaxies in a narrow redshift range around $z \sim 0.2$ to avoid differential evolution.

Our primary sample satisfies (i), (ii) and (iii), and is the subject of our 150 snapshots in cycles 8 and 9. Ten galaxies also satisfy conditions (iv) and (v); these are the cycle 8 targets. The HST observations for four of these have now been completed. We selected the F814W (wide I band) filter. At this wavelength, the light is mostly dominated by old stellar population, so gives a more accurate measure of distortion in the underlying gravitational potential than e.g. UV observations. Details of the current sub-sample are presented in Table 2.

The data were reduced using the Interactive Data Language (IDL), starting from the automatic pipeline products. Cosmic rays were identified as $> 3\sigma$ differences between frames. For sky subtraction, we estimated the modal value of the underlying counts distribution using iterative fits to the readout histograms. The final HST images for the four sub-mJy radio sources are presented in Figure 1.

3 RESULTS

[CM84] 144 is extremely disturbed, with a tidal tail extending $\sim 1.5''$ North-East of the nucleus. Several secondary nuclei are also apparent, reminiscent of HST WFPC2 F814W imaging of ultra-luminous infrared galaxies (e.g. Borne et al. 2000) such as Arp 220 (Borne & Lucas 1997).

[CM84] 074 is only mildly asymmetric. There are hints of face-on spiral structure, and an excess flux $\sim 0.5''$ West of the nucleus. There are two companion galaxies a few arcseconds to the West, also visible in the digitised sky survey. (We reject these as identifications of the radio source based on the ID magnitude quoted in Benn et al. 1993.)

Galaxy Phoenix-Deep-29 is again not as clearly disturbed. However, the inner isophotes are clearly offset in position and (tentatively) in orientation from the outer isophotes. This galaxy also shows signs of interaction with a companion $5''$ to the East. There is a clear tidal tail from the companion extending a few arcseconds North.

Galaxy Phoenix-Deep-96 shows clear signs of morphological disturbance, with the structure dominated by a bright central bar-like feature. There are also hints of multiple nuclei inside the bar, and there is a secondary peak $\sim 0.5''$ South-West of the bar. There are however no other clearly associated companion galaxies visible in the HST image.

To quantify the morphological disturbance, we follow the procedure adopted by Brinchmann et al. (1998) and others, by rotating each image through

π and subtracting it from the original image. Normalising this to the galaxy flux yields the fractional asymmetric flux:

$$A = \frac{\sum |G_{ij} - G'_{ij}|}{\sum G_{ij}} - k \quad (1)$$

where G (G') is the rotated (unrotated) image, k is a correction for systematics such as sky gradients, and the sum is performed over pixels ij . The values of A are fairly insensitive to the choice of aperture used for the self-subtraction, provided all pixels at $\gtrsim 1.5\sigma$ are included in the subimage. The magnitude of k can be estimated by applying the technique to blank sky regions of the same size. The errors in A are in practice dominated by the uncertainty in k : we find typically $\Delta A \simeq 0.05$. A further advantage of this statistic is that the I -selected Canada-France Redshift Survey (CFRS) and b_J -selected LDSS surveys have extensive published HST morphologies quantified using the same statistic, yielding valuable control samples. The asymmetry measures for the sub-mJy star-forming galaxies, quantified as discussed above, are listed in Table 2.

4 DISCUSSION AND CONCLUSIONS

In Figure 2 we plot the asymmetry statistics of our galaxies, and compare them to a control sample of coeval galaxies from the CFRS sample (Brinchmann et al. 1998). The control extends to fainter I_{F814W} fluxes than our star-forming galaxy sample, though there is some overlap. Remarkably, our galaxies are far more asymmetric than the control sample of an (ostensibly) identical population of optically-selected star-forming galaxies of the same I_{F814W} .

The optical control must be well-matched with the radio sample in as many *optical* properties as possible. The radio sample is more asymmetric at a fixed optical luminosity, but is this also true at a fixed optically-derived SFR? I.e., could the morphological differences between the radio sample and the optically-selected control be instead because they are not well-matched in optically-derived star formation rates? To address this we must compare the $H\alpha$ luminosities of our radio sample with those of the control. The data for the radio samples are presented in Benn et al (1993) and Georgakakis et al (2000). The individual $H\alpha$ luminosities of the CFRS galaxies are not published, but Tresse & Maddox (1998) report a tight correlation between $H\alpha$ luminosities and $M_B(AB)$ absolute magnitudes. In Figure 3 we use this relation to estimate the $H\alpha$ -derived star formation rates, and compare the optical control sample with our sub-mJy star-forming galaxies. We adopt the following conversion between $H\alpha$ luminosities and star-formation rates (SFRs):

$$\text{SFR}(H\alpha) = L(H\alpha)/(1.41 \times 10^{34} \text{W}) \quad (2)$$

which is derived assuming Salpeter IMF between $0.1 M_\odot$ and $125 M_\odot$ (see Serjeant et al. 1998, Oliver et al. 1998). We de-redden our $H\alpha$ fluxes by $A_V = 1$ for consistency with optically-selected samples. (Tresse & Maddox 1998 note that the $H\alpha$ luminosity function is essentially unchanged if assuming this A_V throughout their sample, instead of using individual Balmer decrements.) There is a more substantial overlap of the $H\alpha$ -derived SFR with the control sample, and it is again clear that at a *fixed* $H\alpha$ SFR the radio-selected sample is significantly more disturbed than the optically-selected sample of star forming galaxies.

In summary, the radio-selected sources are typically more morphologically disturbed than the optically-selected control, well-matched in redshift, optical luminosity and/or $H\alpha$ SFR. Why this might be the case is hinted in Table 2, where we compare the star formation rates of our galaxies estimated from $H\alpha$ and the 1.4GHz radio luminosity. To convert decimetric radio luminosities to SFRs we use

$$\text{SFR}(1.4\text{GHz}) = L_{1.4}/(7.63 \times 10^{20} \text{W Hz}^{-1}) \quad (3)$$

appropriate for the same IMF as above (see Oliver et al. 1998, Serjeant et al. 1998). Our $H\alpha$ SFRs are comparable in most cases to L_* in the $H\alpha$ luminosity function (Tresse & Maddox 1997). However the radio-derived star formation rates are much larger (though still comparable with the radio L_* , Table 1). This indicates that a large fraction of the star formation in these objects occurs in regions with $A_V \gg 1$, since the observed $H\alpha$ luminosities will be dominated by regions with $A_V \lesssim 1$. Indeed if the dust is well-mixed with the $H\alpha$ emitting gas, the different optical depths for $H\alpha$ and $H\beta$ ensure that $A_V = 1.1$ would be derived for a simple screen Balmer decrement model *regardless* of the true extinction to the rear of the cloud. We therefore suggest that optically-selected samples may under-represent disturbed galaxies with large amounts of obscured star formation, in any SFR-weighted quantity.

The galaxy morphologies of the sub-mJy sources are also markedly different from coeval AGN. McLure et al. (1999) and McLeod & Reike (1995) have found giant ellipticals hosting both radio-loud and radio-quiet quasars at these redshifts, and radiogalaxies are also early type galaxies at these epochs. The EMSS-selected sample of Schade et al. (1999) at $z \leq 0.15$ also finds no evidence for strong interaction/merger activity for any AGN in the sample. This may pose problems for models which propose causal links between the cosmic evolution of AGN and the cosmic star formation history. For example, a model in which both are driven by similar merger events must also provide a mechanism for delaying the onset of central engine fuelling, to account for the (relatively) more relaxed AGN host galaxy potentials. This is related to the more fundamental and unsolved problem of AGN evolution: how to drive the gas fuel down ~ 5 orders of magnitude in radius.

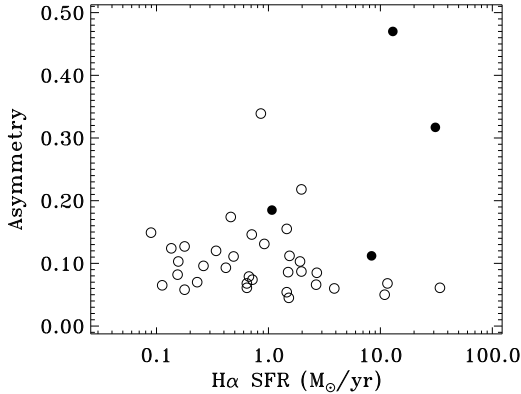


Figure 3. Asymmetry parameter plotted against the estimate of the H α star formation rate discussed in the text. Symbols as in Figure 2.

We can also compare our sample with the ultraluminous galaxy samples of e.g. Borne et al. (2000), who also used HST WFPC2 F814W in snapshot mode. These authors found highly disturbed systems often in moderately rich environments, which they used to argue for an evolutionary sequence involving compact groups and ultraluminous galaxies. Although asymmetry statistics have not been calculated for the ultraluminous galaxies, our targets appear qualitatively less disturbed and the environments possibly less rich. (Ideally both ultraluminous galaxies and radio-selected star-forming galaxies should also have their environments quantified with for example the B_{gg} statistic; e.g. Yee & Green 1984, Hill & Lilly 1991, Wold et al. 2000) This may suggest a link between the level of star formation activity after interactions and the richness of the environment, perhaps via the number or the nature of the interaction events.

Although our current sample is small, the asymmetric morphologies in our $\sim L_*$ targets suggest that galaxy interactions play a major role in the evolution of the star formation and metal production rates in the low- z Universe. Further papers in this series will present results for larger samples of sub-mJy star-forming galaxies. However, it is worth keeping in mind that the formation and evolution of galaxies cannot be characterised by a single parameter, such as the volume-averaged star formation rate. In expanding on this simple first-order description, the obscuration-independent selection of galaxies will be essential, as will co-ordinated multi-wavelength follow-up (e.g. ELAIS, Oliver et al. 2000).

ACKNOWLEDGEMENTS

It is a pleasure to thank Patricia Royle for her help in the preparation of these observations. Based on observations with the NASA/ESA Hubble Space Telescope, obtained at the Space Telescope Science Institute, which is operated by the Association of Universities for Research in Astronomy, Inc. under NASA

contract No. NAS5-26555. This work was supported by PPARC (grant number GR/K98728) and by the EC TMR Network programme (FMRX-CT96-0068).

REFERENCES

- Abraham, R.G., Merrifield, M.R., Ellis, R.J., Tanvir, N.R., Brinchmann, J., 1999, MNRAS 308, 569
 Benn C.R., Rowan-Robinson M., McMahon R.G., Broadhurst T.J. & Lawrence A., 1993, MNRAS, 263, 98
 Borne, K.D., Lucas, R.A., 1997, in preparation
 Borne, K.D., Bushouse, H., Lucas, R.A., Colina, L., 2000, ApJ 529, L77
 Brinchmann, J., et al., 1998, ApJ, 499, 112
 Condon J.J., 1992, ARA&A, 30, 575
 Condon, J.J., Mitchell, J.J., 1984, AJ 89, 610
 Cram, L., 1998, ApJ 506, L85
 Cram L., Hopkins A., Mobasher B. & Rowan-Robinson M., 1998, ApJ 507, 155
 Flores, H., et al. 1999, ApJ 517, 148
 Georgakakis, A., Mobasher, Cram, L., Hopkins, A., Lidman, C. and Rowan-Robinson, M. 2000, MNRAS 306, 708
 Haarsma, D.B., Partridge, R.B., 1998, ApJ, 503, L5
 Hammer F., Crampton D., Lilly S.J., Le Fèvre O. & Kenet T., 1995, MNRAS, 276, 1085
 Hill, G.J., Lilly, S.J., 1991, ApJ 367, 1
 Hopkins, A., et al., 1998 MNRAS 296, 839
 Hopkins, A., et al., 1999 ApJ 519, L59
 Hughes, D., Serjeant, S., Dunlop, J., Rowan-Robinson, M., Blain, A., Mann, R.G., Peacock, J., Efstathiou, A., Gear, W., Oliver, S., Lawrence, A., Longair, M., Goldschmidt, P., Jennes, T., 1998, Nature, 394, 421
 Madau et al. 1996 MNRAS, 283, 1388
 McLeod, K.K., Reike, G.H., 1995, APJL 454, 77
 McLure, R.J., Kukulka, M.J., Dunlop, J.S., Baum, S.A., O’Dea, C.P., Hughes, D.H., 1999, MNRAS 308, 377
 Meurer, G., Heckman, T., Lenhart, M.D., Leihner, C., Lowenthal, J., 1997, AJ 114, 54
 Mitchell, K.J., Condon, J.J., 1985, AJ 90, 1957
 Oliver, S., Gruppioni, C., Serjeant, S., 1998, preprint (astro-ph/9808260)
 Oliver, S., et al., 2000, MNRAS in press
 Oort, J.A., 1987, A&AS 71, 221
 Pettini, M., et al., 1998, ApJ 508, 539
 Rowan-Robinson, M., et al., 1993, MNRAS 263, 123
 Rowan-Robinson M. et al., 1997, MNRAS, 289, 490
 Schade, D., Boyle, B.J., Letawsky, M., 1999, preprint astro-ph/9912294
 Serjeant, S., Gruppioni, C., Oliver, S., 1998, preprint (astro-ph/9808259)
 Steidel, C.C., et al. 1996, ApJ 462, L17
 Steidel, C.C., et al. 1999, ApJ 519, 1
 Tresse, L., Maddox, S.J., 1998, ApJ 495, 691
 Windhorst R.A., Fomalont E.B., Kellermann K.I., Partridge R.B., Richards E., Franklin B.E., Pascarella S.M. & Griffiths R.E., 1995, Nature, 375, 471
 Wold, M., Lacy, M., Lilje, P.B., Serjeant, S., 2000, MNRAS in press (astro-ph/9912070)
 Yee, H.K.C., Green, R.F., 1984, ApJ 280, 79